


EPTT-2020-0037

**NUMERICAL INVESTIGATION OF THE NATURAL VENTILATION
INFLUENCE IN THE THERMAL COMFORT OF AN INDUSTRIAL SHED**

Douglas Pereira Vasconcellos*


 Polytechnic School, Pontifícia Universidade Católica do Paraná, Curitiba, PR 80215-901, Brazil

 *douglasvasconcellos@yahoo.com.br

Michel Nikolaos Stamoulis[†]

Gerson Henrique dos Santos[‡]

Luiz Eduardo Melo Lima[§]

 Department of Mechanics, Federal University of Technology—Paraná—, Ponta Grossa, PR 84017-220, Brazil

 [†]michelstamoulis@hotmail.com, [‡]gsantos@utfpr.edu.br, [§]lelima@utfpr.edu.br

Abstract. *Research seeking strategies for energy efficiency in buildings has been encouraged, because of a greater need for conscious energy consumption, due to the latest energy crises and environmental demands. As a way to achieve thermal comfort in environments, the thermal insulation application in the envelope, and the development of architectural projects that use natural convection, were studied in several types of research. Hence, this work aims to analyze the influence of the cross ventilation application on the thermal comfort of an industrial building (shed), considering the annual average wind in the city of Ponta Grossa, PR, Brazil. The ANSYS[®] Fluent[®] commercial software, a computational fluid dynamics tool, was used to solve the governing equations that model this problem, i.e., Reynolds-averaged Navier–Stokes. For the turbulence modeling, the standard k – ϵ model was used, which is a two-equation model: one for turbulent kinetic energy and another for its dissipation rate. The industrial shed analyzed has a simple industrial park and no bulkheads, with the building oriented in the north–south direction and having doors with a large proportion concerning the envelope area. From the results of the average of the internal velocities obtained for the airflow velocity fields, the cross ventilation application in the industrial shed proved to be satisfactory for improving the environment’s thermal comfort according to literature. Also, stagnation regions occurred close to the industrial shed walls, whose influence can be minimized, provided that thermal insulation is applied to reduce the heat exchange of the wraps.*

Keywords: numerical simulation, cross ventilation, thermal comfort

1. INTRODUCTION

The oil crisis in the 1980s brought a greater need for energy savings and, consequently, a reduction in energy consumption in buildings, especially those used commercially and industrially. The reduction of energy consumed in heating, ventilation, and air-conditioned (HVAC) systems is one of the most important steps to reduce the total demand for global energy (Baniassadi *et al.*, 2016; Baniassadi and Sailor, 2018).

The concept of energy efficiency in buildings refers to enabling thermal comfort for users with low energy consumption (Lamberts *et al.*, 2014). Therefore, one building is more efficient than another, when in the same environmental condition, it has lower energy consumption. Fanger *et al.* (1974) carried out studies through statistical analysis that indicate people’s preferences concerning thermal conditions. Their work resulted in the development of two indices: the predicted mean vote (PMV) and the predicted percentage of dissatisfied (PPD). PMV consists of the mean vote of a large people number with a sensations scale, called the seventh scale, whose value ranges from -3 to 3 , with zero being the value attributed to the neutral. PPD is used to indicate the percentage of people dissatisfied according to their desire for a warmer, colder, or even maintained environment.

Research conducted by Humphreys and Fergus Nicol (2002) suggests that PMV tends to overestimate the heat sensation for airflow velocities up to 0.2 m/s. On the other hand, according to the data collected from users, the cooling capacity is underestimated when there is an increase in airflow velocity (Nicol, 1995). The effective temperature expresses the combined effect of air temperature, relative humidity, radiation, and air movement that provide an identical thermal sensation (Koenigsberger, 1974). When there is ventilation, the thermal sensation is of an environmental temperature different from the real one (effective temperature). For example, in a situation where the dry bulb temperature is 28 °C, wet bulb temperature is 25 °C, and airflow velocity is 0.5 m/s, an individual has an air temperature sensation of 25.5 °C (Barbirato *et al.*, 2007).

The comfort condition in naturally ventilated environments depends on the temperature and velocity of the air. Also, in places where the wind is stable in terms of direction and has a reasonable velocity value ($> 3 \text{ m/s}$), the ventilation provided by the wind force is the simple and most efficient cooling strategy (Santamouris, 2004). Also, fluctuations in airflow velocity, characterized by the turbulence intensity, increase the airflow and affect thermal comfort (Koskela *et al.*, 2001). Cross ventilation can be employed to increase the thermal comfort of users in the environments, as it favors heat exchanges by convection and evaporation. Also, it minimizes the use of mechanical refrigeration devices and, consequently, reduces energy consumption in these spaces (Bastide *et al.*, 2006). The discomfort caused by the turbulence resulting from a constant airflow can occur in cold, temperate climates, where individuals are not used to continuous air movement. Figure 1 shows the effects of the wind velocity and turbulence intensity on the thermal comfort sensation.

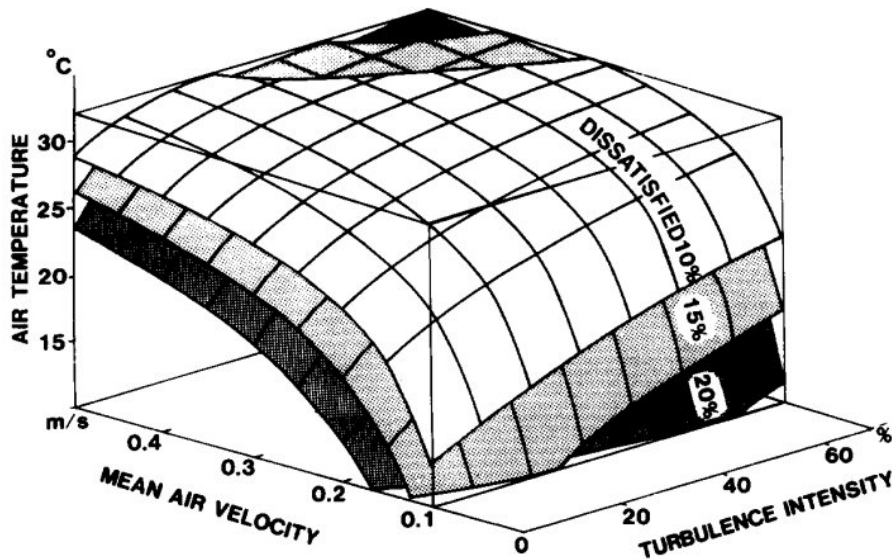


Figure 1. Thermal confort sensation as a function of the wind velocity and turbulence intensity (Fanger *et al.*, 1988).

An analysis of the association between velocity and distribution of the airflow can help to improve the thermal comfort. Because considering only the mean velocity values, it is not possible to predict the occurrence of areas where the airflow is stagnant to the detriment of others where there is a concentration of streams with higher velocity values, as a consequence of the distribution of the openings in the building, as shown in Fig. 2.

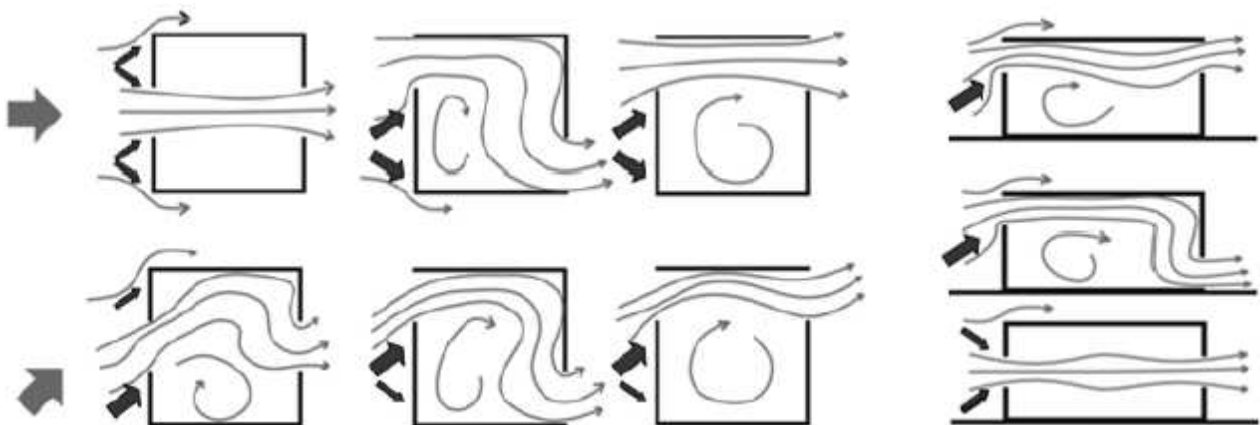


Figure 2. Effect of the distribution of the openings in a building on the airflow (Givoni, 1998).

In this context, this work aims to analyze the influence of the cross ventilation application on the thermal comfort of an industrial shed, considering the annual average wind in the city of Ponta Grossa, PR, Brazil. One commercial software for computational fluid dynamics (CFD) was employed to solve the governing equations that model this problem. The results should demonstrate the occurrence of the stagnant zones of the airflow within the industrial shed.

2. MODEL

This section presents the definitions of the governing equations (Sect. 2.1) and the turbulence model (Sect. 2.2) for the computational model employed in this work.

2.1 Governing equations

Equations (1), (2), and (3) are the RANS equations and express the conservation of mass, momentum, and energy, respectively, in steady-state for incompressible flow (Tannehill *et al.*, 1997):

$$\frac{\partial \bar{u}_j}{\partial x_j} = 0 \quad (1)$$

$$\frac{\partial}{\partial x_j} (\rho \bar{u}_i \bar{u}_j + \hat{p} \delta_{ij} - \bar{\tau}_{ij}^{\text{tot}}) = 0 \quad (2)$$

$$\frac{\partial}{\partial x_j} [(\rho C_p \bar{T} - \hat{p}) \bar{u}_j - \bar{\tau}_{ij}^{\text{tot}} \bar{u}_i + \bar{q}_j^{\text{tot}}] = 0 \quad (3)$$

Where x_i and \bar{u}_i represent the position and velocity vectors, respectively, δ_{ij} is the Kronecker delta function, ρ is the density, C_p is the isobaric specific heat, and \bar{T} is the absolute temperature.

The modified pressure \hat{p} has its definition given by Eq. (4):

$$\hat{p} = \bar{p} + \rho g x_i \quad (4)$$

Where g is the gravitational acceleration. For an ideal gas, the static pressure is provided by $\bar{p} = \rho R \bar{T}$, with R being the gas constant.

The total (laminar and turbulent) viscous stress, $\bar{\tau}_{ij}^{\text{tot}}$, and the total (laminar and turbulent) heat flux, \bar{q}_j^{tot} , are given by Eqs. (5) and (6), respectively:

$$\bar{\tau}_{ij}^{\text{tot}} \equiv \bar{\tau}_{ij}^{\text{lam}} + \bar{\tau}_{ij}^{\text{turb}} = (\mu + \mu_t) \left(\frac{\partial \bar{u}_i}{\partial x_j} + \frac{\partial \bar{u}_j}{\partial x_i} \right) \quad (5)$$

$$\bar{q}_j^{\text{tot}} \equiv \bar{q}_j^{\text{lam}} + \bar{q}_j^{\text{turb}} \approx -C_p \left(\frac{\mu}{\text{Pr}} + \frac{\mu_t}{\text{Pr}_t} \right) \frac{\partial \bar{T}}{\partial x_j} \quad (6)$$

Where μ and μ_t are the molecular and turbulent dynamic viscosities, respectively, and Pr and Pr_t are the laminar and turbulent Prandtl numbers, respectively. For air $\text{Pr} \approx 0.71$, and a turbulence model is used to give values for μ_t as well as Pr_t , although $\text{Pr}_t \approx 0.9$ is usually employed.

2.2 Turbulence model

The standard k - ϵ turbulence model proposed by Launder and Spalding (1974) consists of the two transport equations. The first for the turbulent kinetic energy k , Eq. (7), and the second for its dissipation rate ϵ , Eq. (8):

$$\frac{\partial}{\partial t} (\rho k) + \frac{\partial}{\partial x_j} \left[\rho k u_j - \left(\mu + \frac{\mu_t}{\sigma_k} \right) \frac{\partial k}{\partial x_j} \right] = P_k + P_b - Y_{\text{Ma}} - \rho \epsilon \quad (7)$$

$$\frac{\partial}{\partial t} (\rho \epsilon) + \frac{\partial}{\partial x_j} \left[\rho \epsilon u_j - \left(\mu + \frac{\mu_t}{\sigma_\epsilon} \right) \frac{\partial \epsilon}{\partial x_j} \right] = C_{1\epsilon} (P_k + C_{3\epsilon} P_b) \frac{\epsilon}{k} - C_{2\epsilon} \rho \frac{\epsilon^2}{k} \quad (8)$$

Where σ_k and σ_ϵ are the turbulent Prandtl numbers for k and ϵ , respectively, and these constants are in Table 1. For steady-state, the time derivatives in Eqs. (7) and (8) can be eliminated, i.e., $\partial/\partial t = 0$.

The turbulent viscosity, μ_t , is calculated by combining k and ϵ , according to Eq. (9):

$$\mu_t = C_\mu \rho \frac{k^2}{\epsilon} \quad (9)$$

Where C_μ is a constant, and its value is in Table 1.

The kinetic energy production term due to the mean velocity gradients, P_k , is given by Eq. (10):

$$P_k = -\overline{\rho u'_i u'_j} \frac{\partial u_j}{\partial x_i} \equiv \mu_t S^2 \quad (10)$$

Where S ($\equiv \sqrt{2S_{ij}S_{ij}}$) is the modulus of the mean rate-of-strain tensor considering the Boussinesq hypothesis, i.e., $S_{ij} = (1/2)(\partial u_i/\partial x_j + \partial u_j/\partial x_i)$.

The kinetic energy production term due to buoyancy, P_b , is given by Eq. (11):

$$P_b = g_i \beta \frac{\mu_t}{Pr_t} \frac{\partial T}{\partial x_i} \quad (11)$$

Where g_i is the gravitational acceleration vector. For the standard k - ϵ model, the Pr_t default value is 0.85. By definition, the thermal expansion coefficient is $\beta = -(1/\rho)(\partial \rho/\partial T)_p$. For isothermal flow, the kinetic energy production term due to buoyancy can be eliminated, i.e., $P_b = 0$.

The dilatation dissipation term, Y_{Ma} , is modeled by Eq. (12), according to Sarkar and Lakshmanan (1991):

$$Y_{Ma} = 2Ma_t^2 \rho \epsilon \quad (12)$$

Where the turbulent Mach number is defined as $Ma_t = \sqrt{k/a^2}$, by definition, and a ($\equiv \sqrt{\gamma RT}$, for an ideal gas) is the speed of sound, with γ being the specific heats' ratio, and R is the gas constant. For incompressible flow, the dilatation dissipation term can be eliminated, i.e., $Y_{Ma} = 0$.

Table 1 presents the default values of the coefficients in the standard k - ϵ model selected in the computational tool.

Table 1. Default values of the coefficients in the standard k - ϵ model.

$C_{1\epsilon}$	$C_{2\epsilon}$	$C_{3\epsilon}$	C_μ	σ_k	σ_ϵ
1.44	1.92	a	0.09	1.0	1.3

^a $0 \leq C_{3\epsilon} \leq 1$, but an approximation that satisfies both limits is $C_{3\epsilon} = \tanh |v/u|$, where v and u are the velocity components parallel and perpendicular to the gravitational vector, respectively (Henkes *et al.*, 1991).

3. NUMERICAL PROCEDURE

The commercial software ANSYS® Fluent® Release 18.0 was employed to run the numerical simulations in this work. All steady-state simulations were performed using a finite volume method (Patankar, 1980) with a structured and uniform mesh. The pressure–velocity coupling was solved using the semi-implicit method for pressure linked equations (SIMPLE) algorithm (Patankar, 1980). The “Enhanced Wall Treatment” option was selected that provides consistent solutions for all y^+ values and is recommended when using the k - ϵ turbulence model for general single-phase fluid flow problems (ANSYS, 2017). The following schemes have been considered in the simulations performed:

- Second-order for pressure.
- Second-order upwind for momentum.
- First-order upwind for turbulent kinetic energy and its dissipation rate.

All simulations are performed in the Computational Research Laboratory, linked to the Graduate Program in Mechanical Engineering of the Federal University of Technology—Paraná—, using a computer with the following characteristics:

- Microsoft Windows® 7 (64-bit) operating system.
- Intel® Core™ i7–3770 (3.4 GHz) processor.
- 8 GB RAM.

The following sections introduce the descriptions and characteristics of the industrial building geometry (Sect. 3.1) and computational mesh and boundary conditions (Sect. 3.2), considered in the numerical procedure.

3.1 Industrial shed geometry

In this work, we considered a turbulent flow occurring in an industrial warehouse with a total area of 300 m², located in the region of Ponta Grossa, PR, Brazil. In this locality, the average annual winds correspond to a airflow velocity of 3.5 km/h with peaks of 4.5 km/h and 5 km/h. Cross ventilation occurs through two metal gates with an area of 12 m² located on the opposite walls of the industrial shed, as shown in Fig. 3. On the parallel walls of the industrial shed, there are 20 m² glazed areas (closed and infiltration-free windows). The industrial shed geometry was created in the ANSYS® SpaceClaim® tool. Table 2 shows the industrial shed characteristics dimensions.

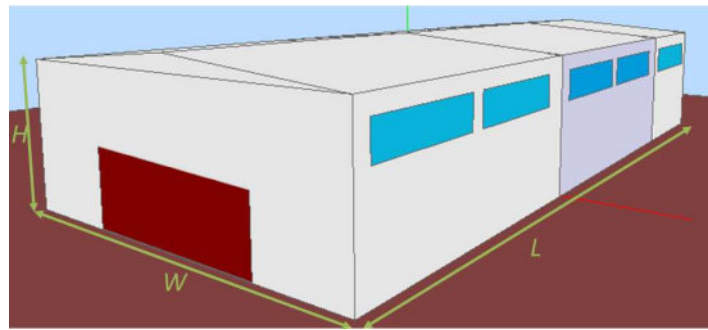


Figure 3. Industrial shed geometry.

Table 2. Industrial shed characteristics dimensions.

L (m)	W (m)	H (m)	\bar{U} (m ³)	A_{floor} (m ²)	A_{gates} (m ²)	A_{glazed} (m ²)
25	12	5	1500	300	24	40

3.2 Computational mesh and boundary conditions

The ANSYS® Meshing™ tool was applied to generate the computational meshes. Three meshes are created for the three-dimensional (3D) computational domain showed in Fig. 3: (a) a coarse mesh with 950 nodes and 648 elements; (b) a medium mesh with 5032 nodes and 4032 elements; (c) a fine mesh with 23374 nodes and 20496 elements. The three meshes are showed in Fig. 4. The fine mesh showed results similar to the medium mesh with a maximum deviation of less than 1%; also, the simulation times were very close. Thus, this work employed the fine mesh.

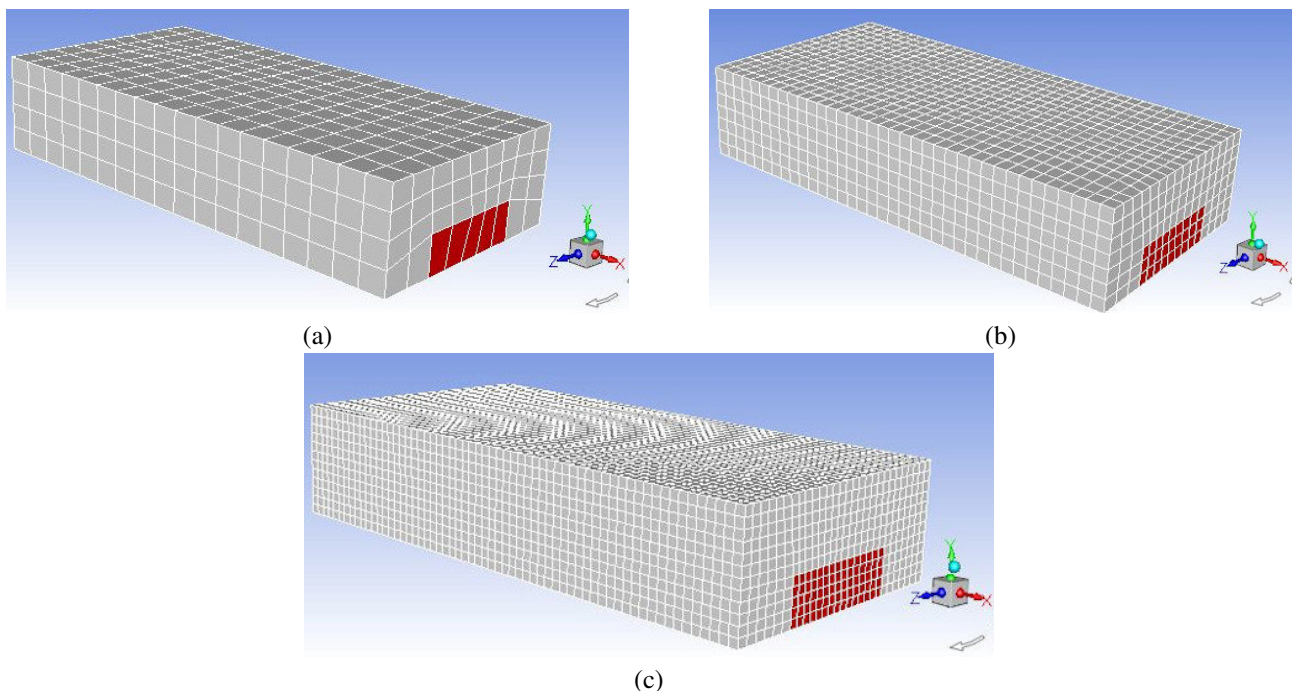


Figure 4. 3D computational meshes analyzed: (a) coarse mesh; (b) medium mesh; (c) fine mesh.

The wind performs an internal flow in the industrial shed, which is south-north direction positioned, and the south and north faces gates are the control volume inlet and outlet, respectively. It was also supposed that the roof and the floor are adiabatic surfaces, as it contains a thermal insulator, leaving only the walls of the building envelope available for thermal exchange with the external environment. These surfaces have an initial temperature of 310 K, already admitted in previous works considering the climatic archive of the Ponta Grossa region for the annual average temperature (Mendes *et al.*, 2003). The internal airflow was supposed to be in steady-state, fully developed, with no external pressure at the flow outlet and turbulent regime for the velocities of 1.5 m/s, 2.5 m/s, and 3.5 m/s at the inlet gate, that correspond to Cases A, B, and C, respectively.

4. RESULTS AND DISCUSSION

Figure 5 presents the simulation results for the Case A of the inlet velocity of 1.5 m/s. These results show the behavior of the streamlines (Fig. 5a) and for velocity vectors (Fig. 5b).

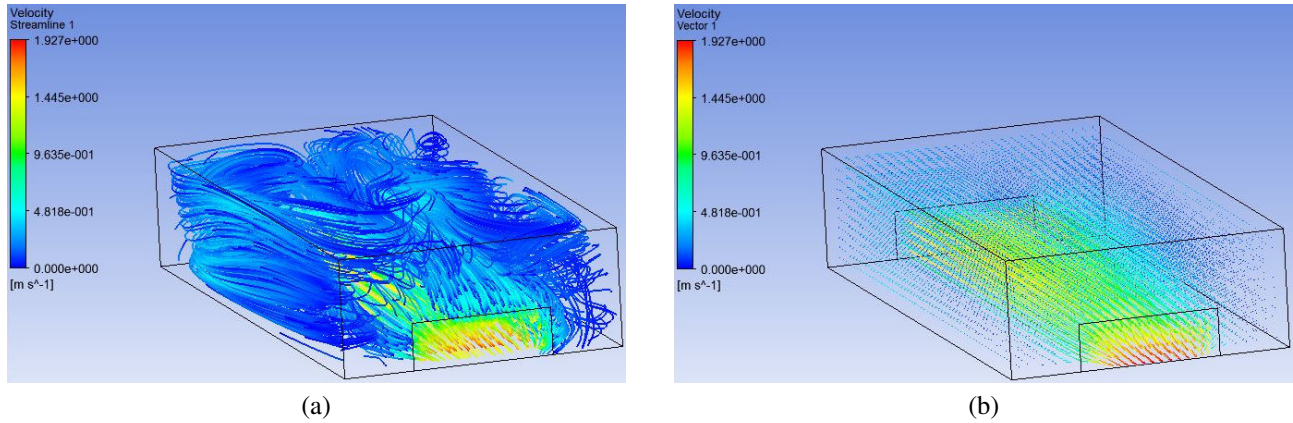


Figure 5. Simulation results for 1.5 m/s (Case A): (a) streamlines and (b) velocity vectors.

Figure 6 presents the simulation results for the Case B of the inlet velocity of 2.5 m/s. These results show the behavior of the streamlines (Fig. 6a) and for velocity vectors (Fig. 6b).

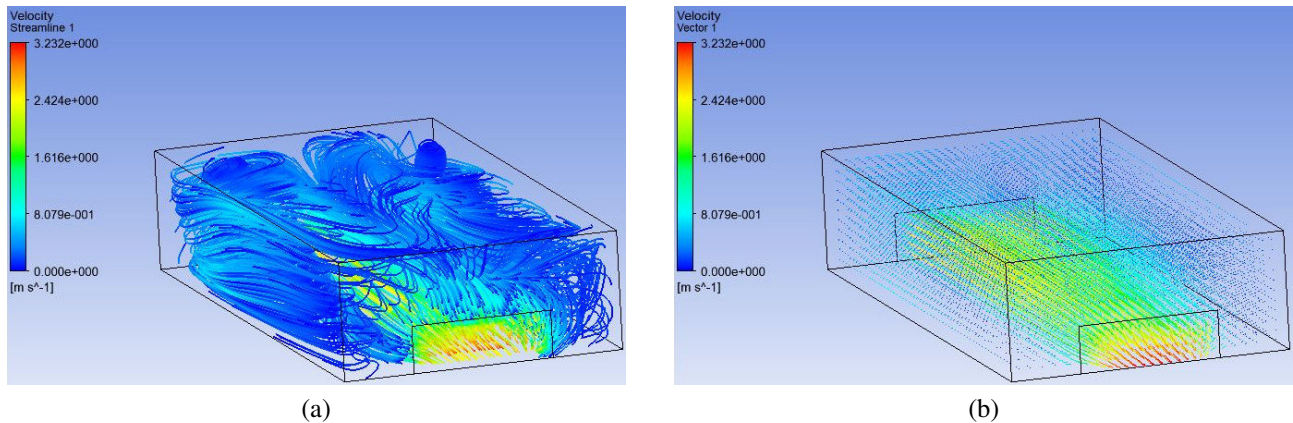


Figure 6. Simulation results for 2.5 m/s (Case B): (a) streamlines and (b) velocity vectors.

Figure 7 presents the simulation results for the Case C of the inlet velocity of 3.5 m/s. These results show the behavior of the streamlines (Fig. 7a) and for velocity vectors (Fig. 7b).

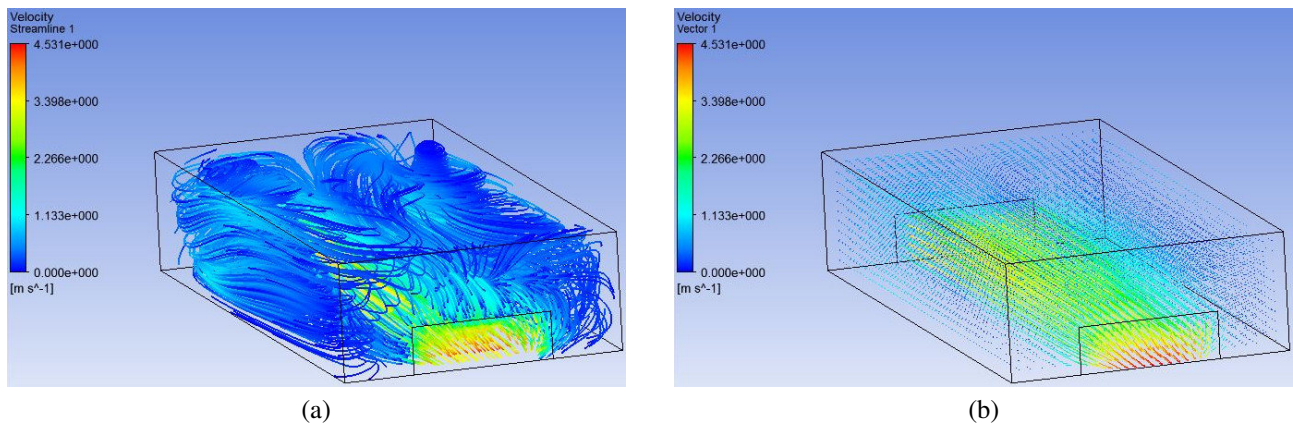


Figure 7. Simulation results for 3.5 m/s (Case C): (a) streamlines and (b) velocity vectors.

In Figures 5, 6, and 7 (Cases A, B, and C, respectively), it is possible to observe the occurrence of stagnation regions, especially near the corners of the industrial shed. On the other hand, the central area along the shed shows the highest

velocities values, as previously discussed in the literature. Regarding the distribution of the internal air velocity, there is symmetry in the flow. And this occurs due to the symmetry inlet and outlet openings of the air.

The average of the internal velocities obtained for the three cases analyzed (inlet velocities of 1.5 m/s, 2.5 m/s, and 3.5 m/s) are 0.452 m/s, 0.759 m/s, and 1.067 m/s, respectively. In terms of these average of the internal velocities, the first two cases analyzed (inlet velocities of 1.5 m/s and 2.5 m/s) are within the thermal comfort limits established for Brazil (0.8 m/s for the average of the internal velocities), according to Givoni (1992) and ASHRAE (2017). Therefore, there is an inlet velocity value between 2.5 m/s and 3.5 m/s (Cases B and C, respectively) that exceeds this established limit for the average of the internal velocities in the building. Besides, the three cases analyzed have inlet velocity values that are higher than the average annual winds in the analyzed region. Similar results were obtained by Mazon (2005) in a ventilation analysis in industrial sheds with skylights using CFD.

5. CONCLUSIONS

The influence of the cross ventilation applied on the thermal comfort of an industrial shed was analyzed in this work, considering the annual average winds in the city of Ponta Grossa, PR, Brazil.

From the results obtained for the airflow velocity fields, the cross ventilation application in the industrial shed proved to be satisfactory for improving the environment's thermal comfort as long as the flow profile inside the industrial shed is maintained, depending on the inlet velocity value. Also, stagnation regions occurred close to the industrial shed walls, whose influence can be minimized, provided that thermal insulation is applied to reduce the heat exchange of the wraps. The results obtained from the simulations performed are following the literature and contribute to the thermal comfort analysis of the industrial sheds.

The next steps in this study consist of an analysis of the temperature profiles, considering different types of thermal insulators applied to the building walls, as well as variations in the configurations of the building's inlet and outlet.

6. ACKNOWLEDGEMENTS

The authors thank the Federal University of Technology—Paraná—and the Pontifícia Universidade Católica do Paraná for the resources made available.

7. REFERENCES

- ANSYS, 2017. *ANSYS Fluent Tutorial Guide*. ANSYS, Inc., Canonsburg, PA. Release 18.0.
- ASHRAE, 2017. *ANSI/ASHRAE Standard 55-2017: Thermal Environmental Conditions for Human Occupancy*. American National Standards Institute (ANSI), American Society of Heating, Refrigerating and Air-Conditioning Engineers (ASHRAE), Tullie Circle NE; Atlanta, GA.
- Baniassadi, A. and Sailor, D.J., 2018. "Synergies and trade-offs between energy efficiency and resiliency to extreme heat – A case study". *Build. Environ.*, Vol. 132, pp. 263–272. ISSN 0360-1323. DOI 10.1016/j.buildenv.2018.01.037.
- Baniassadi, A., Sajadi, B., Amidpour, M. and Noori, N., 2016. "Economic optimization of PCM and insulation layer thickness in residential buildings". *Sustainable Energy Technol. Assess.*, Vol. 14, pp. 92–99. ISSN 2213-1388. DOI 10.1016/j.seta.2016.01.008.
- Barbirato, G.M., Souza, L.C.L.d. and Torres, S.C., 2007. *Clima e Cidade: a Abordagem Climática como Subsídio para Estudos Urbanos*. EdUFAL, Maceió, AL. ISBN 9788571773592. In Portuguese.
- Bastide, A., Lauret, P., Garde, F. and Boyer, H., 2006. "Building energy efficiency and thermal comfort in tropical climates". *Energy Build.*, Vol. 38, No. 9, pp. 1093–1103. ISSN 0378-7788. DOI 10.1016/j.enbuild.2005.12.005.
- Fanger, P.O., Melikov, A.K., Hanzawa, H. and Ring, J., 1988. "Air turbulence and sensation of draught". *Energy Build.*, Vol. 12, No. 1, pp. 21–39. ISSN 0378-7788. DOI 10.1016/0378-7788(88)90053-9.
- Fanger, P.O., Ostergaard, J., Olesen, S. and Madsen, T.L., 1974. "The effect on man's comfort of a uniform air flow from different directions". *ASHRAE Trans.*, Vol. 80, No. 2, pp. 142–157. ISSN 0001-2505. ASHRAE Annual Conference, Montreal, QB.
- Givoni, B., 1992. "Comfort, climate analysis and building design guidelines". *Energy and Buildings*, Vol. 18, No. 1, pp. 11–23. ISSN 0378-7788. DOI 10.1016/0378-7788(92)90047-k.
- Givoni, B., 1998. "Effectiveness of mass and night ventilation in lowering the indoor daytime temperatures. Part I: 1993 experimental periods". *Energy Build.*, Vol. 28, No. 1, pp. 25–32. ISSN 0378-7788. DOI 10.1016/S0378-7788(97)00056-X.
- Henkes, R.A.W.M., Van Der Vlugt, F.F. and Hoogendoorn, C.J., 1991. "Natural-convection flow in a square cavity calculated with low-Reynolds-number turbulence models". *Int. J. Heat Mass Transfer*, Vol. 34, No. 2, pp. 377–388. ISSN 0017-9310. DOI 10.1016/0017-9310(91)90258-G.
- Humphreys, M.A. and Fergus Nicol, J., 2002. "The validity of ISO-PMV for predicting comfort votes in every-day thermal environments". *Energy Build.*, Vol. 34, No. 6, pp. 667–684. ISSN 0378-7788. DOI 10.1016/S0378-7788(02)00018-X.

- Koenigsberger, O.H., ed., 1974. *Manual of Tropical Housing and Building: Climatic Design*. Longman, London. ISBN 9780582445451.
- Koskela, H., Heikkinen, J., Niemelä, R. and Hautalampi, T., 2001. “Turbulence correction for thermal comfort calculation”. *Build. Environ.*, Vol. 36, No. 2, pp. 247–255. ISSN 0360-1323. DOI 10.1016/S0360-1323(00)00002-0.
- Lamberts, R., Dutra, L. and Pereira, F.O.R., 2014. *Eficiência Energética na Arquitetura*. ELETROBRAS/PROCEL, Rio de Janeiro, RJ, 3rd edition. In Portuguese.
- Lauder, B.E. and Spalding, D.B., 1974. “The numerical computation of turbulent flows”. *Comput. Methods Appl. Mech. Eng.*, Vol. 3, No. 2, pp. 269–289. ISSN 0045-7825. DOI 10.1016/0045-7825(74)90029-2.
- Mazon, A.A.O., 2005. *Ventilação natural em galpões utilizando lanternins*. Master’s thesis, Universidade Federal de Ouro Preto, Ouro Preto, MG. URL <http://www.repositorio.ufop.br/handle/123456789/2240>. In Portuguese.
- Mendes, N., Oliveira, R.C.L.F. and dos Santos, G.H., 2003. “Domus 2.0: a whole-building hygrothermal simulation program”. In *Proceedings of the Eighth International IBPSA Conference*. International Building Performance Simulation Association (IBPSA), Eindhoven, Vol. 8 of *Building Simulation 2003*, pp. 863–870. URL http://www.ibpsa.org/proceedings/bs2003/bs03_0863_870.pdf.
- Nicol, F., ed., 1995. *Standards for Thermal Comfort: Indoor Air Temperature Standards for the 21st Century*. Chapman & Hall, London; New York, 1st edition. ISBN 9780419204206.
- Patankar, S.V., 1980. *Numerical Heat Transfer and Fluid Flow*. Series in Computational Methods in Mechanics and Thermal Sciences. Hemisphere Publ. Co., New York, NY, 1st edition. ISBN 9780891165224.
- Santamouris, M., 2004. “Natural ventilation in urban areas”. *Ventilation Information Paper*, Vol. 1, No. 3, pp. 3:1–3:10.
- Sarkar, S. and Lakshmanan, B., 1991. “Application of a Reynolds stress turbulence model to the compressible shear layer”. *AIAA J.*, Vol. 29, No. 5, pp. 743–749. ISSN 1533-385X. DOI 10.2514/3.10649.
- Tannehill, J.C., Anderson, D.A. and Pletcher, R.H., 1997. *Computational Fluid Mechanics and Heat Transfer*. Series in Computational and Physical Processes in Mechanics and Thermal Sciences. Taylor & Francis Group, Washington, DC, 2nd edition. ISBN 9781560320463.

8. RESPONSIBILITY NOTICE

The authors are the only responsible for the printed material included in this paper.